3D microstructure and damage accumulation in a cast AlSi12Cu5Ni2 piston alloy as a function of solution treatment

Katrin Bugelnig[1], Frederico Sket[2], Holger Germann[3], Thomas Steffens[3], Fabian Wilde[4], E. Boller[5], Guillermo Requena[6]

[1]Institute of Materials Science and Technology, Technical University of Vienna, Karlsplatz 13/308, A-1040 Vienna, Austria, email: katrin.bugelnig@tuwien.ac.at

[2]IMDEA Materials , C/ Eric Kandel 2, 28906 Getafe, Spain

[3] KS Kolbenschmidt GmbH, Karl-Schmidt-Straße, 74172 Neckarsulm, Germany

[4]Helmholtz-Zentrum Geesthacht, Zentrum für Material- und Küstenforschung GmbH, Max-Planck-Straße 1, 21502 Geesthacht, Germany[5] ESRF-The European Synchrotron, CS40220, Grenoble Cedex 9, France

[6] German Aerospace Centre, Linder Höhe, 51147 Cologne, Germany, e-mail: guillermo.requena@dlr.de

Abstract

The microstructural evolution as well as the damage mechanisms and accumulation during RT tensile deformation of an AlSi12Cu5Ni2 piston alloy for high performance diesel truck engines are studied as a function of solution heat treatment (ST) time at 500°C. For this, interrupted in-situ synchrotron tomography experiments are combined with conventional metallography investigations. The study shows that the lower resistance to structural damage of the alloy after ST is linked to the local disintegration of the highly interconnected 3D network formed by intermetallics and Si embedded in the Al-matrix.

Keywords: Al-Si piston alloys, synchrotron tomography, solution treatment, 3D microstructure, damage evolution

1 Introduction

Nowadays Al alloys are highly demanded for a number of components in automotive applications due to their light weight, thermal and electrical conductivity, good processability and corrosion resistance. Near eutectic Al-Si alloys show excellent castability, good wear resistance and low thermal expansion, which makes them a favorable choice for pistons in high performance diesel truck engines [1]. Pistons are a vital part of the engine and happen to be one of the most thermo-mechanically stressed parts of the entire vehicle. Thus, they are continuously subject of further development for optimization and adaption to new engines with ever higher efficiencies. Particularly, the piston bowl rim has to withstand compressive and tensile stresses at temperatures up to 400°C [2]. The microstructure of these alloys is formed by interconnected 3D hybrid networks of eutectic and primary Si as well as intermetallic phases embedded in a relatively soft α-Al matrix [3]. These networks can undergo topological changes during thermal treatments that influence the thermo-mechanical performance of the alloys. It is therefore necessary to gain micromechanistic understanding of the effect of microstructural features on damage mechanisms and damage evolution in these alloys. The formation and accumulation of damage in this type of alloys is characterized by the formation of micro-cracks

that can propagate and lead to failure during further loading. Contrarily to ductile damage, which normally takes place as a massive bulk phenomenon, this type of damage occurs in a localized manner and, as such, 2D investigations are insufficient to univocally identify or even find crack initiation sites (low number density of cracks). Non-destructive in-situ X-ray synchrotron tomography can solve this problem and, furthermore, the eutectic Si and the α-Al which possess similar X-ray attenuations can be revealed due to the higher achievable phase contrast.
The aim of this study is to characterize the changes in the 3D microstructure of an AlSi12Cu5Ni2 piston alloy during ST and to analyze their influence on damage accumulation studied by synchrotron tomography during interrupted in-situ tensile tests.

2 Experimental Methods

An AlSi12Cu5Ni2 alloy produced by gravity die casting in the form of pistons was studied in the present work. All samples were taken from the bowl rim area of diesel pistons. The alloy was investigated after 0h and after 4h ST at 500°C and was then aged for 5h at 250°C and overaged for 100 hours at 300°C in both conditions. The evolution of microstructure during ST was studied for the same sample after 0h and 4h ST by high resolution synchrotron tomography at the beamline ID19 at the European Synchrotron Radiation Facility (ESRF), Grenoble [4]. The identification of intermetallic phases after ST was conducted using target metallography as shown in [5]. Interrupted in-situ RT tensile tests were carried out at the beamline P05 of PETRA III, DESY, Hamburg [6]. Table 2 presents the experimental conditions during tomography.

Table 2: Beamlines, conducted experiments and Measurementparameters

Beamline:	**Experiment:**	**Energy: [keV]**	**Voxel-Size: [µm^3]**	**Sample to detector distance: [mm]**	**Exposure time: [msec/proj]**	**Nr. of Proj.:**
ID19	Solution Heat Treatment (0h/500°C vs. 4h/500°C)	19	0.3	~3	300	2000
				16	300	
P05	Interrupted in-situ tensile (0h/500°C vs. 4h/500°C)	25	1.2	30	1100	900

Figure 1 shows the sample geometry (Fig. 1a) as well as the experimental setup (Fig. 1b) used for these experiments.

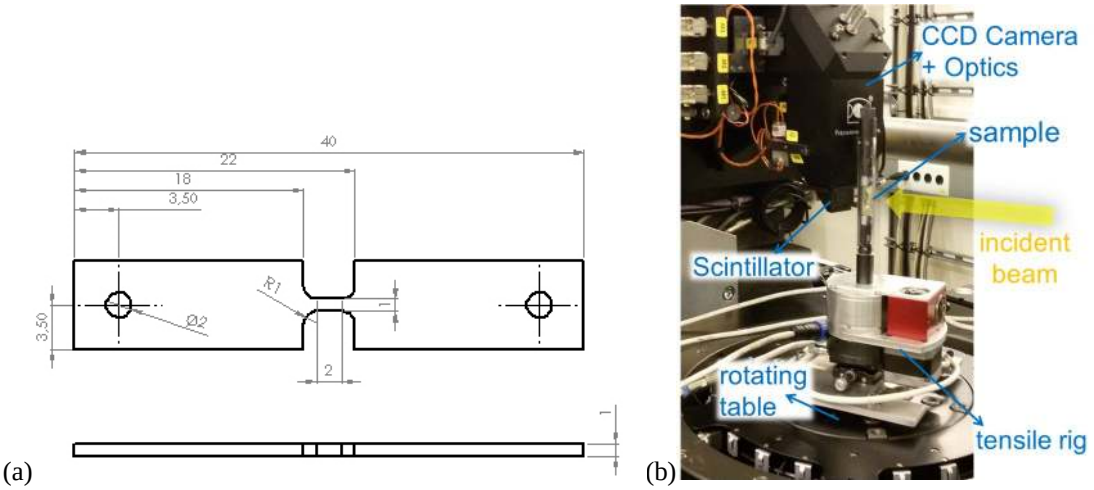

(a) (b)

Figure 1: interrupted in-situ tensile experiments at PETRA III/P05: (a) sample geometry (b) experimental setup.

The fracture surface of post mortem samples was analyzed by light optical microscopy (LOM) and SEM.
Image pre-processing, registration and further processing/quantification/3D visualisation were carried out using the imaging softwares Avizo Fire 8.1, VG StudioMax, MedInria and Fiji.

3 Results and Discussion

Figure 2 shows the microstructure of the investigated alloy in 0h ST condition acquired by LOM . The microstructure consists of bulky primary and plate-like eutectic silicon (darkest phases), and aluminides (bright phases) embedded in the comparatively soft α-Al matrix. SEM/EDX Mappings revealed the presence of a number of different rigid intermetallic phases (see Figure 3 a,b).

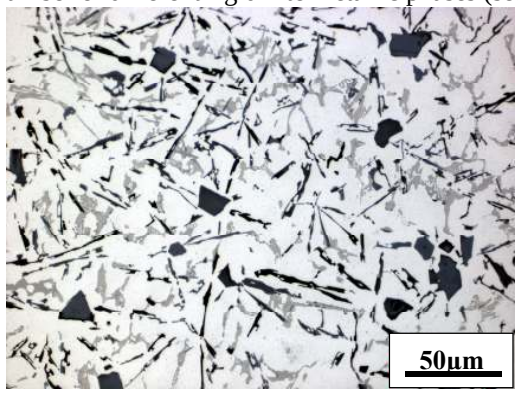

Figure 2: LOM: 2D microstructure of the AlSi12Cu5Ni2 alloy in 0h ST condition.

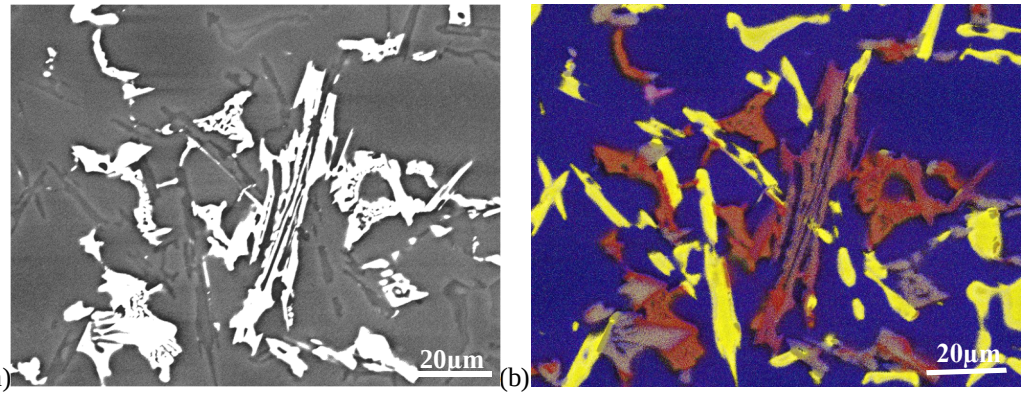

Figure 3: LOM: 2D microstructure of the AlSi12Cu5Ni2 alloy in 0h ST condition: a) SEM micrograph, b) EDX mapping with Al matrix (blue), Si (yellow), Zr, V, Ti (pink), AlCu2 (dark red), AlCuNi (script-like, light red), AlFeNi (violett), AlFeSiNiCuMn (platelike, light red).

Figure 4 displays reconstructed 2D tomographic slices of the same region of the same sample at 0h ST and after 4h ST. Partial dissolution and morphological changes of aluminides (see white particles in Figure 5 (a,c) and (b,d)) as well as slight coarsening and spheroidization of Si particles (dark grey particles in Figure 5 (a,c)) caused a partial loss of connectivity between these rigid phases during ST. Quantitative results show a decrease in volume fraction of about ~1vol% and interconnectivity of aluminides of about ~7 %. Furthermore, the topological parameter Euler number of the aluminides, which describes the changes in local connectivity of 3D networks, increases with progressing ST time indicating a loss of connecting branches within the network.

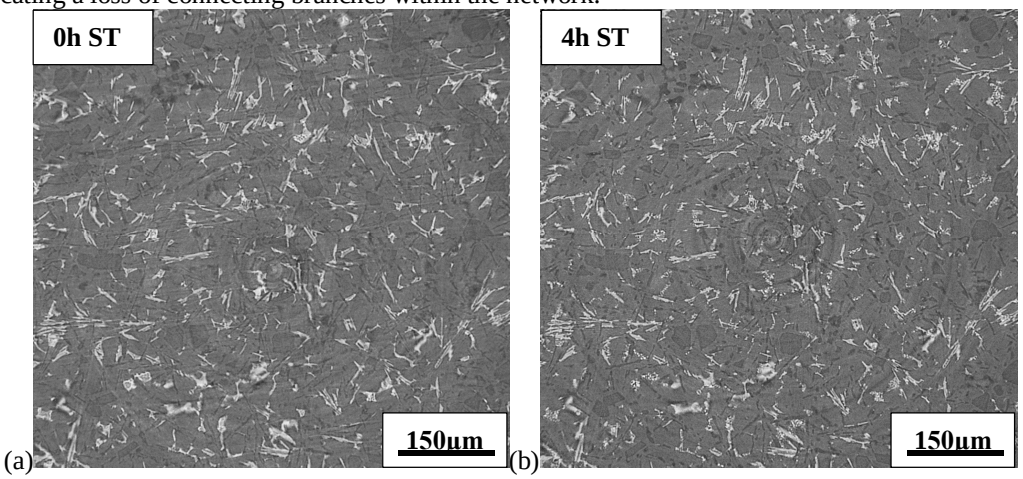

Figure 4: 2D reconstructed slices of the microstructure of the AlSi12Cu5Ni2 alloy (a) 0h ST and (b) after 4h ST.

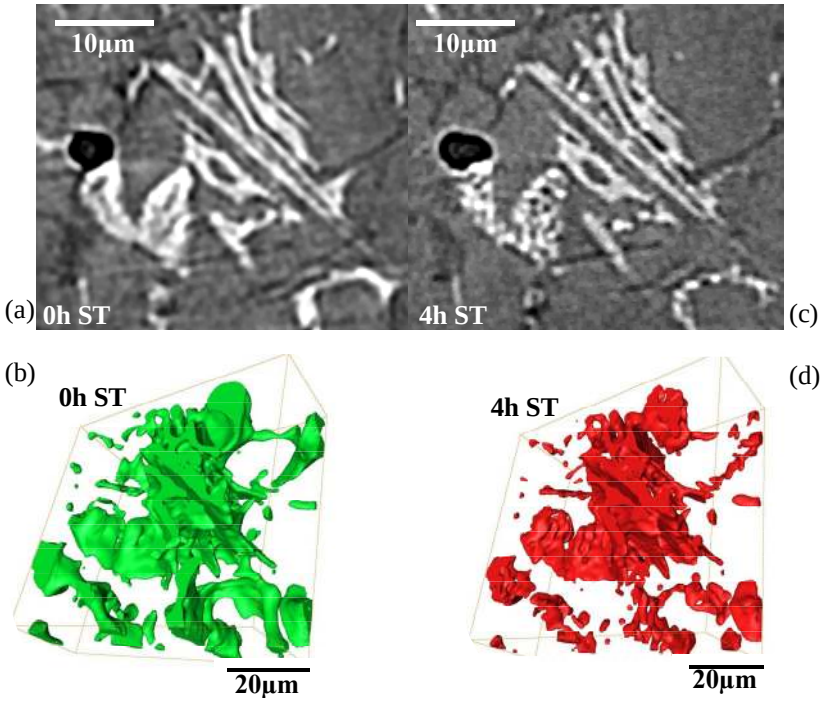

Figure 5: dissolution/loss of local connectivity of aluminides. 2D reconstructed slices of the material after (a) 0h ST and (c) 4h ST and 3D visualization of the in (a,c) presented aluminides after (b) 0h and (d) 4h ST. Investigated volume: 55x55x20µm³, vox. size (0.28µm)³.

The effect of solution heat treatment and the resulting morphological and topological changes of the microstructural compounds were extensively studied, e.g. [7], reporting the dissolution of Cu rich aluminides and the coarsening of Si particles which are similar observations to the current study.
As it can be seen in Figure 6, the stress-displacement curve of the alloy in 0h ST condition shows a very brittle behavior, while the alloy after 4h ST displays some strain hardening . After 0h ST fracture occurred at 215MPa and a displacement of 380µm, while failure of the material after 4h ST occurred a little later, i.e. at ~200MPa and 400µm displacement.

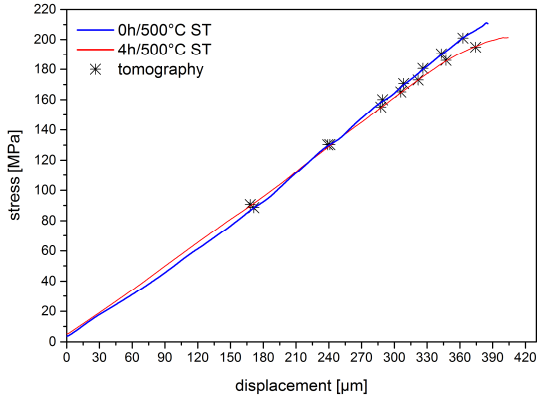

Figure 6: Stress-Displacement Curves of interrupted in-situ tensile experiments after 0h/500°C (blue) and after 4h/500°C Solution Heat Treatment (red); the starmarks indicate the conditions at which synchrotron tomography was conducted.

A significantly higher damage accumulation is detected during RT tensile deformation in 4h ST condition before final failure of the samples (see Figure 7 (a-b)). Damage in the 4h ST condition occurs by micro-crack formation in primary Si particles and aluminides already at 90MPa and 130MPa, respectively, while damage in the 0h ST alloy is observed shortly before failure at about 170MPa (see Figure 8 and 9).

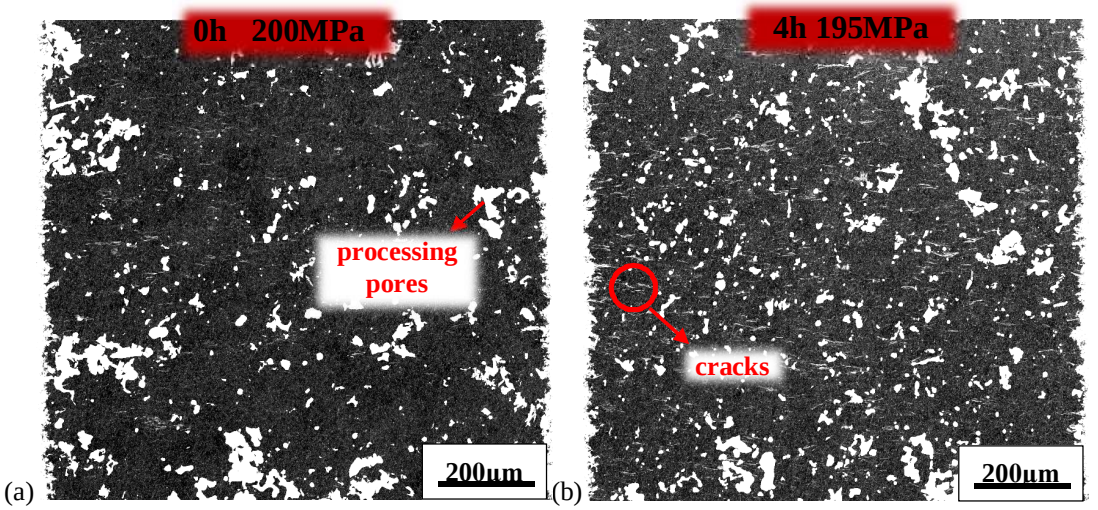

Figure 7: Minimum intensity projection over the full tomographic volume at the last load step before failure of the alloy in (a) 0h and (b) 4h ST conditions. The load direction is vertical.

The dominant damage mechanism in both conditions is a mixture of cracking of primary Si particles and debonding between Si and matrix. Figures 8 and 9 show representative examples of cracking and debonding of Si particles and also cracking of aluminides in a final state of the experiment. Figure 10 (a and b) display 3D visualisations of the in Figure 8 and 9 presented microstructures after 0h and 4h ST, respectively.

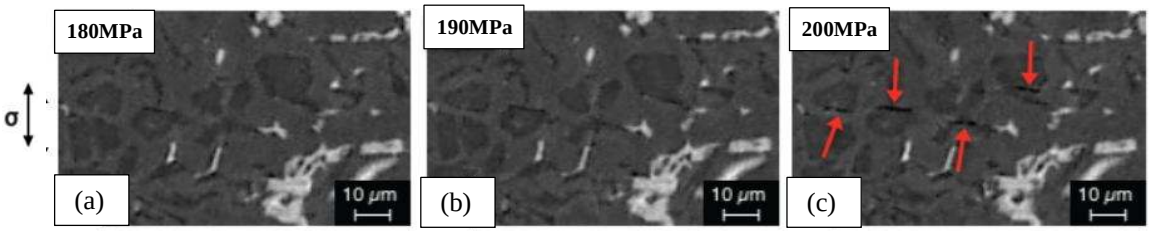

Figure 8: debonding between matrix and Si and micro-crack initiation through primary Si particles and evolution over several load steps of the material after 0h ST. The load direction is vertical.

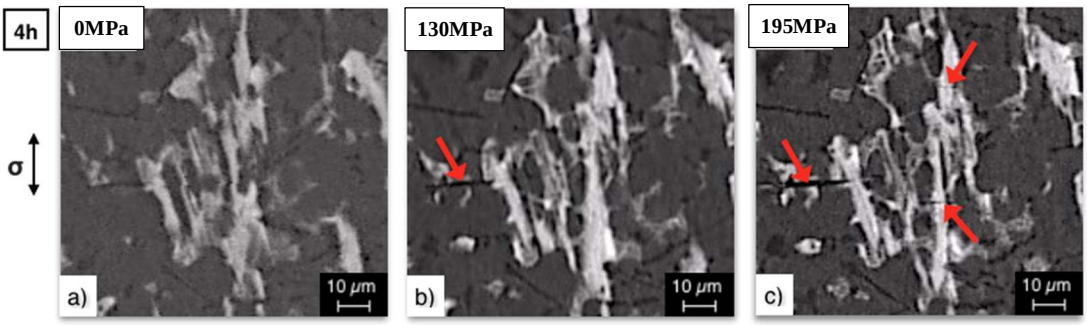

Figure 9: cracking of Si particles and aluminides and evolution over several load steps of the material after 4h ST. The load direction is vertical.

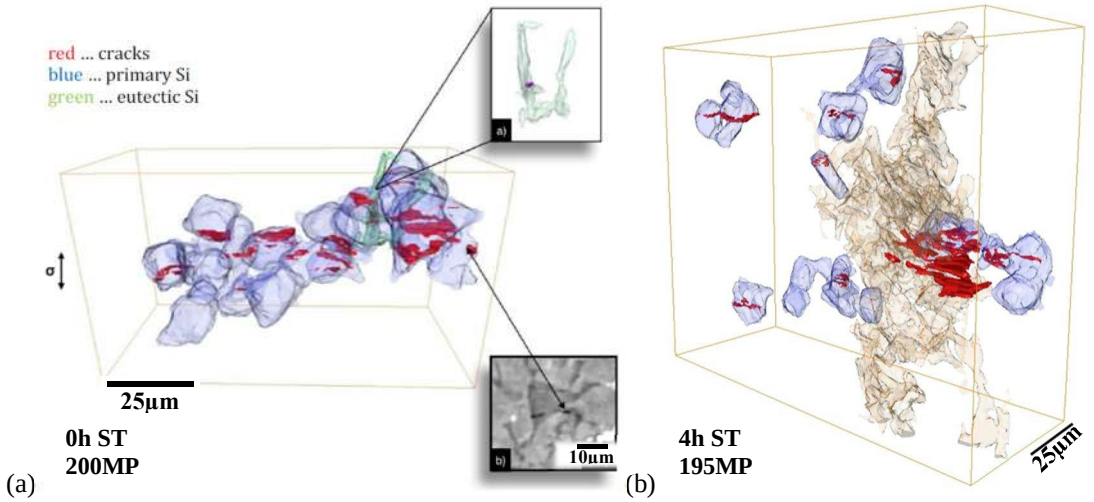

(a) (b)

Figure 10: 3D visualisation of damage mechanisms: (a) cracks (red) in 0h ST codnition; cracks through prim./eutectic Si (blue/green), (b) cracks through aluminides (beige) and Si. The Al-matrix is transparent in both figures. The load direction is vertical.

The difference in load carrying capacity and damage accumulation to failure of the material at 0h ST and after 4h ST is often attributed to the change in matrix hardness, e.g. [8]. However, while a sudden drop in macrohardness from 85±2.3HB(1/10) to 71±0.6HB(1/10) was documented, no changes in matrix-nanohardness could be detected. The macrohardness and strength of the alloy depends on the interconnectivity of rigid phases as well as the matrix hardness [9,10]. The results presented in this work indicate that the loss of connectedness of the aluminides provokes a loss of load carrying capability of the 3D network of Si and aluminides. This leads to a decrease of strength and an increase of the ductility of the alloy in 4h ST condition and to the different damage behaviours between the alloy in 0h and 4h ST conditions.

4 Conclusion

It is concluded that ST time at 500°C has a significant effect on the 3D microstructure of the studied alloy. The tensile behavior of the AlSi12Cu5Ni2 alloy is closely linked to the changes in connectedness of the rigid 3D network of aluminides and Si. Thus, the loss of connecting branches

within this network owing to dissolution of aluminides and spheroisization of Si particles decreases its load bearing capability. This results in earlier damage intiation for the ST condition and, consequently, the strength of the alloy decreases while ductility increases.

Acknowledgements

The ESRF and DESY are acknowledged for the provision of synchrotron facilities at the beamlines ID19 and P05, respectively. The authors acknowledge the financial support by the "K-Project for Non-Destructive Testing and Tomography Plus".

References

[1] T.O. Mbuya, I. Sinclair, A.J. Moffat, P.A.S. Reed, Micromechanisms of fatigue crack growth in cast aluminum piston alloys, International Journal of Fatigue, Vol 42, pp. 227-237, 2012.

[2] F.S. Silvia, Fatigue on engine pistons – a compendium of case studies, Engineering Failure Analysis, Vol 13, pp. 480-492, 2006.

[3] Z. Asghar, G. Requena, E. Boller, 3D rigid multiphase networks providing high-temperature strength to cast AlSi10Cu5Ni1-2 piston alloys, Act. Mat. 59, pp. 6420-6432, 2011.

[4] European synchrotron radiation facility <http://esrf.fr>

[5] R. Fernández Gutiérrez, G. Requena, B. Stauder, 3D-Characterization of AlCu5Mg0.3Mn0.3 and AlCu7Mn0.4 Alloys, Pract. Metall.: Vol. 51, No. 6, pp. 451-462, 2014.

[6] DESY Photon Science, PETRA III http://petra3.desy.de/

[7] M. Lebyodkin, A. Deschamps, Y. Bréchet, Influence of second phase morphology and topology on mechanical and fracture properties if Al-Si alloys, Materials Science and Engineering A 234-236 (1997), pp. 481-484.

[8] M. Schöbel, G. Baumgartner, S. Gerth, J. Bernardi, M. Hofmann, Microstresses and crack formation in AlSi7MgCu and ALSi17Cu4 alloys for engine components, ActaMaterialia, Vol 81, pp. 401-408, 2014.

[9] D.Tolnai, G. Requena, P. Cloetens, J. Lendvai, H.P. Degischer, Effect of Solution treatment on the internal architecture and compressive strength of an AlMg4,7Si alloy, Materials Science & Engineering A, Vol. 585, pp. 480-487, 2013.

[10] G. Requena, G. Garcés, Z. Asghar, E. Marks, P. Staron, P. Cloetens, The Effect of Connectivity of Rigid Phases on Strength of Al-Si Alloys, Advanced Engineering Materials, Vol. 13, pp. 674-684, 2011.